

Supramolecular Structures of Trimethylphenylammonium Cation Crystallized with Iodide and Hydrogen Sulfate Anions

Qutaiba Abu-Salem^{a*}, Basem F. Ali^{a,b}

^a Department of Chemistry, Faculty of Science, University of Al al-Bayt, Al-Mafraq 25113, Jordan

^b Department of Chemistry, King Faisal University, Ahsa 31982, Saudi Arabia

Received on Jun. 14, 2016

Accepted on Nov. 6, 2016

Abstract

The structures of two salts of trimethylphenylammonium cation with iodide (**1**) and hydrogen sulfate (**2**) have been determined at 173 K. Crystals of both **1** and **2** are in the orthorhombic space groups $P2_12_12_1$ and $Pna2_1$, with $Z = 4$ and cell dimensions $a = 5.7671(7)$, $b = 7.9353(6)$ and $c = 22.258(2)$ for **1** and $a = 9.3995(10)$, $b = 13.0661(13)$ and $c = 8.9860(13)$ Å for **2**. In **1**, the trimethylphenylammonium cation is hydrogen bonded and is restricted to non-classical $H_2C-H...I$ and $(\pi)C-H...(\pi)$ hydrogen bonds. The presence of hydrogen sulfate in **2** allowed further classical ($O-H...O$) and non-classical ($C-H...O$, $H_2C-H...(\pi)$ and $(\pi)C-H...(\pi)$) hydrogen bonding. Consequently, lattices of both **1** and **2** form supramolecular structures.

Keywords: *Trimethylphenylammonium cation; O—H...O, H₂C—H...I, C—H... π and aryl...aryl interactions; Supramolecular structure.*

Introduction

Extensive research has been devoted to explore and understand intermolecular interactions. These are assorted into different types^[1, 2] such as hydrogen bonding,^[3-5] $X...X$ ($X = \text{halogen}$) interactions,^[6, 7] aryl...aryl interactions,^[8] $X...aryl$ ^[9] and $C-H...aryl$ interactions.^[10] Among above mentioned interactions, hydrogen bonding is the most common and influential. Hydrogen bonding includes both classical ($D-H...A$; D: donor, A: acceptor with donor and acceptor atoms being N, O and F) and non-classical interactions where the donor and acceptor atoms are extended to include other atoms (e.g. $C-H...O$, $C-H...X$ and $C-H...(\pi)$ interactions). The weakest amongst these interactions is the $C-H...(\pi)$ interaction which is of special interest because of its many implications.^[11-15] The significance of this topic stems from our interest in the solid state chemistry of the aryl salts formed by the $4-Me_3NC_6H_4X$ ($X = H, I, Hg$) fragment.^[16-18] Supramolecular contacts formed by hydrogen bonds are considered as powerful tool to examine the crystal packing of the molecular or extending building blocks.^[19] Herein, we report the crystal structures of trimethylphenylammonium iodide (**1**) and trimethylphenylammonium hydrogen sulfate (**2**), along with an analysis of the supramolecular aspects of these crystal structures.

* Corresponding author: e-mail: q.abusalem@gmail.com

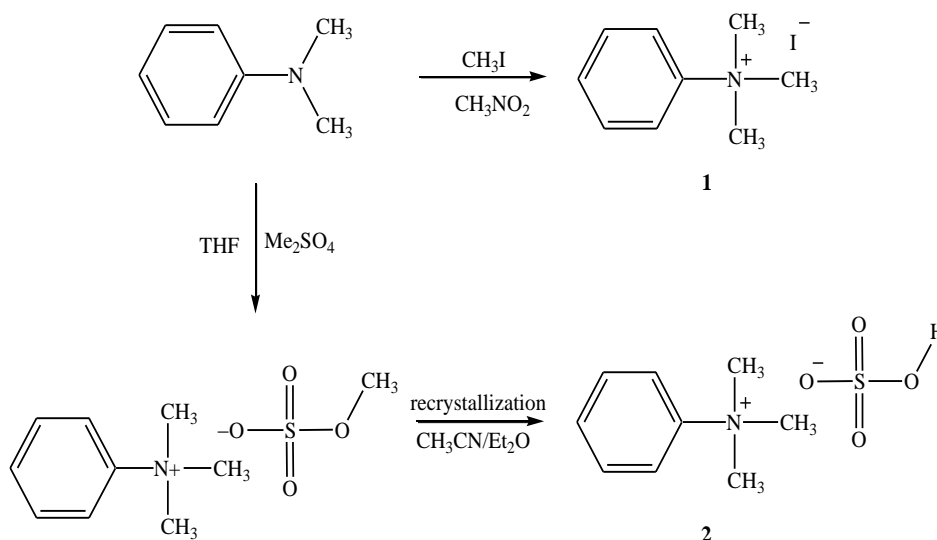
Experimental

Materials and physical measurements

Chemicals were purchased from Aldrich and used as received. The high resolution NMR spectra were acquired by a Bruker DRX 400 NMR spectrometer (^1H 400 MHz; ^{13}C 100 MHz, using TMS as external standard). The elemental analysis for C, H and N were performed using a Carlo Erba 1106 elemental analyzer.

Synthesis

The synthesis and crystallization of both salts are outlined in scheme 1. Detailed procedures are given below.



Scheme 1: Synthesis and crystallization of the title compounds.

Synthesis of trimethylphenylammonium iodide [$\text{Me}_3\text{NC}_6\text{H}_5]^+ \text{I}^-$ (1)

CH₃I (2.35 g, 16.5 mmol) was added to a solution of Me₂NC₆H₅ (2.00 g, 16.5 mmol) in CH₃NO₂ (35 mL) with stirring for 24 h at room temperature. The product was then precipitated by adding Et₂O, filtered, washed with Et₂O and dried in vacuum. Yield: 3.83 g (88%). The obtained solid was recrystallized from EtOH/Et₂O as colourless crystals. NMR (DMSO-*d*₆): ^1H δ = 3.66 (s, 9H, NCH₃), 7.59-8.02 (m, 5H_{aryl}); ^{13}C δ = 56.40 (NCH₃), 120.4 (C₂), 130.0 (C₃), C₄ (N/O), 147.2 (C₁). Anal. Calcd. for C₉H₁₄IN (Mwt. = 263.11): C, 41.08; H, 5.36; N, 5.32. Found: C, 41.03; H, 5.16; N, 5.22%. MS (FAB +ve.): *m/z* (%) = 136.1 (100).

Synthesis of trimethylphenylammonium methylsulfate [$\text{Me}_3\text{NC}_6\text{H}_5]^+ \text{MeOSO}_3^-$

Me₂SO₄ (1.56 g, 12.4 mmol) was added to a solution of Me₂NC₆H₅ (1.50 g, 12.4 mmol) in THF (30 mL) with stirring for 24 h at room temperature. The resulting solid was filtered, washed with Et₂O and dried in vacuum. Yield: 2.14 g (70%). NMR (DMSO-*d*₆): ^1H δ = 3.38 (s, 3H, CH₃O), 3.61 (s, 9H, NCH₃), 7.57-7.98 (m, 5H_{aryl}); ^{13}C δ = 52.80 (CH₃OSO₃), 56.30 (NCH₃), 120.4 (C₂), 130.0 (C₃), C₄ (N/O), 147.2 (C₁). Anal. Calcd. for C₁₀H₁₇NO₄S (Mwt. = 247.09): C, 48.56; H, 6.93; N, 5.66; Found: C, 48.49; H,

6.88; N, 5.57%. MS (FAB +ve.): m/z (%) = 136.1 (100) and (FAB -ve.): m/z (%) = 110.9 (100) (MeOSO₃⁻).

Synthesis and crystallization of trimethylphenylammonium hydrogensulfate [Me₃NC₆H₅]⁺HOSO₃⁻ (2)

Upon recrystallization of [Me₃NC₆H₅]⁺MeOSO₃⁻ from CH₃CN/Et₂O, colourless crystals of **2** were obtained.

X-ray crystallography

A crystal of compound **1** or **2** was mounted on a glass fiber with epoxy cement at room temperature and cooled in a cold stream of liquid nitrogen. The intensity data of the two salts were collected using a STOE IPDS 2 diffractometer with graphite-monochromated Mo K α radiation (λ = 0.71073 Å) at 173 K. The structures were solved by direct methods and refined by full-matrix least-square procedures on F^2 with the SHELX-97 and SHELXL-97 programs.^[20] All non-hydrogen atoms were refined anisotropically and were added on calculated positions. The details of data collection, refinement and crystallographic data are summarized in Table 1.

Table 1: Crystal data and structure refinement for **1** and **2**.

Compound	1	2
Empirical formula	C ₉ H ₁₄ IN	C ₉ H ₁₅ NO ₄ S
Formula mass	263.11	233.28
Temperature (K)	173(2)	173(2)
Crystal system	Orthorhombic	Orthorhombic
Space group	<i>P</i> 2 ₁ 2 ₁	<i>P</i> na2 ₁
Unit cell dimension (Å)		
<i>a</i>	5.7671(7)	9.3995(10)
<i>b</i>	7.9353(6)	13.0661(13)
<i>c</i>	22.258(2)	8.9860(13)
Volume, Å ³	1018.6(2)	1103.6(2)
<i>Z</i>	4	4
Calculated density, (mg/ m ³)	1.716	1.404
μ (mm ⁻¹)	3.087	0.288
F(000)	512	496
Crystal size (mm ³)	0.2 x 0.1 x 0.05	0.30 x 0.30 x 0.05
range for data collection (°)	3.15–26.37	3.50–29.28
Index ranges (<i>h</i> , <i>k</i> , <i>l</i>)	-7/7, -9/9, -27/27	-12/12, -17/16, -12/12
Reflections collected	14600	19324
Independent reflection	2080 ($R_{int} = 0.0376$)	2983 ($R_{int} = 0.0886$)
Data/ restraints/ Parameters	2080 / 0 / 100	2983 / 1 / 196
Goodness-of-fit on F^2	1.106	1.203
Final <i>R</i> indices [$I > 2\sigma(I)$]	$R_1 = 0.0167$, $wR_2 = 0.0372$	$R_1 = 0.0606$, $wR_2 = 0.1258$
Final <i>R</i> (all data)	$R_1 = 0.0191$, $wR_2 = 0.0379$	$R_1 = 0.0745$, $wR_2 = 0.1317$
$\Delta\rho_{max/min}$ (e·Å ⁻³)	0.326/ -0.342	0.293 / -0.468

Results and Discussion

Synthesis and crystallization

The quaternary salts **1**^[21] and $[\text{Me}_3\text{NC}_6\text{H}_5]^+\text{MeOSO}_3^-$ were synthesized in good yields by alkylating the tertiary amine $\text{Me}_2\text{NC}_6\text{H}_5$ in CH_3NO_2 and THF, respectively, for 24 h at room temperature using CH_3I and Me_2SO_4 as alkylating agents. Single crystals of **1** were obtained by vapor diffusion of diethylether into the ethanol solution of the compound at room temperature for one day. Spectroscopic characterization (see experimental section) confirmed the afforded salts. However, the recrystallization of $[\text{Me}_3\text{NC}_6\text{H}_5]^+\text{MeOSO}_3^-$ salt by vapor diffusion of diethylether into acetonitrile solution allowed unexpectedly the hydrolysis into **2**, as confirmed unambiguously by its x-ray structure.

NMR Spectra

The ^1H NMR spectra of $[\text{Me}_3\text{NC}_6\text{H}_5]^+\text{I}^-$ and $[\text{Me}_3\text{NC}_6\text{H}_5]^+\text{MeOSO}_3^-$ are consistent with the proposed structures. In DMSO, the protons for the phenyl ring exhibited chemical shifts in the range 7.57-8.02 ppm as multiplet. The *N*-methyl protons signal was observed in the range 3.61-3.66 ppm, while the singlet at 3.38 ppm was attributed to MeOSO_3^- anion protons in $[\text{Me}_3\text{NC}_6\text{H}_5]^+\text{MeOSO}_3^-$.

The ^{13}C NMR spectrum of $[\text{Me}_3\text{NC}_6\text{H}_5]^+\text{MeOSO}_3^-$ has displayed, in addition to the expected resonances for the phenyl ring carbons in the range 120.4-147.2 ppm, two signals: One for the $\text{N}(\text{CH}_3)_3$ carbons at 56.3 ppm and another signal at 52.8 ppm assigned to the carbon of MeOSO_3^- anion. The ^{13}C NMR spectrum of **1** is also in agreement with the suggested structure and the resonances for the phenyl ring and $\text{N}(\text{CH}_3)_3$ carbons lie within the range as in $[\text{Me}_3\text{NC}_6\text{H}_5]^+\text{MeOSO}_3^-$.

Molecular structure

The structures of the title compounds **1** and **2** are presented in Figure 1. The cation fragment in both salts has bond lengths and angles that are comparable with literature averages for TMPA^+ containing salts, for example, bis(trimethylphenylammonium) $[\mu]$ -oxalato-bis[oxidodiperoxidomolybdate(VI)],^[22] trimethylphenylammonium $[\mu]$ -bromido-bis[dibromidobis(4-bromobenzyl)stannate(IV)],^[23] bis(trimethylphenylammonium) tetrabromidocuprate(II),^[24] bis(trimethylphenylammonium) hexabromide /chloride (0.792/0.208) stannate(IV),^[25] catena-poly[bis(trimethylphenylammonium) [hexa- $[\mu]$ -chlorido-dichloridotricuprate(II)]],^[26] trimethylphenylammonium dibromidotriphenylstannate(IV)^[27], trimethyl(4-iodophenyl)ammonium iodide^[17] and bis(trimethyl(4-mercuryphenyl)ammonium tetraiodomercurate(II)).^[18] The geometrical dimensions of the bisulfate anion are also within the reported values as in phenazin-5-ium hydrogen sulfate monohydrate,^[28] 8-hydroxyquinolin-1-ium hydrogen sulfate monohydrate,^[29] 8-hydroxy-5,7-dimethylquinolin-1-ium hydrogensulfate^[30] and 3-(4-Methoxyphenyl)-1,3-selenazol[2,3-b][1,3]benzothiazol-4-ium hydrogen sulfate.^[31] Selected geometrical parameters for both salts are listed in Table 2.

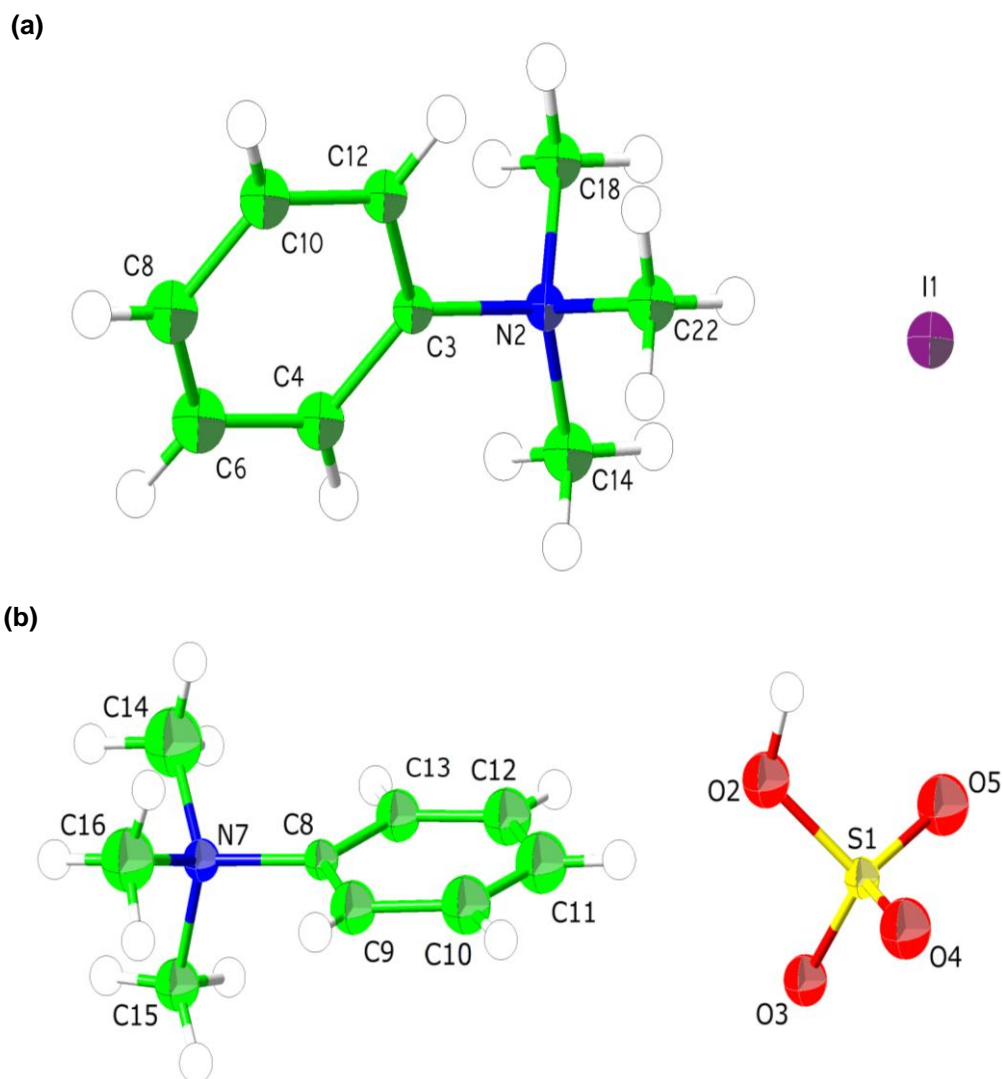


Fig. 1: Molecular structures of: (a) $[\text{TMPA}]^+\text{I}^-$ (**1**) and (b) $[\text{TMPA}]^+\text{HOSO}_3^-$ (**2**) with the atomic numbering scheme; thermal ellipsoids drawn at the 50% probability level.

Supramolecular hydrogen-bonding synthons in $[\text{TMPA}]^+\text{X}^-$; $\text{X} = \text{I}, \text{HOSO}_3$

The supramolecular hydrogen-bonding synthons (Scheme 2) in $[\text{TMPA}]^+\text{X}^-$; $\text{X} = \text{I}, \text{HOSO}_3$, are shown in Figs. 2-5. The structural data for those contacts which are considered to be viable hydrogen-bonds are listed in Table 3. In compound **1**, the main component in the structure is the cation part with the interactions being aryl...aryl intermolecular interactions with C–H... π contact (2.788 Å) in an edge-to-face supramolecular motif (Scheme 2, Synthon **A**). The geometrical parameters of this pertinent interatomic interaction are summarized in Table 3. On the other hand, the cation...iodide ($\text{H}_2\text{C}-\text{H}\dots\text{I}$) interaction forms non-classical C–H...I contacts (3.079 and 3.093 Å) with a single halide atom (Scheme 2, Synthon **B**). In compound **2**, a particularly significant feature of the synthons (**C** to **G**) is the fact that one of the CH groups of the phenyl ring (para position to N) forms bifurcated C–H...O contacts (Scheme 2, synthon **C**) with the bisulfate anion (2.646-2.655 Å).

Table 2: Selected geometrical parameters (Å, °) for **1** and **2**.

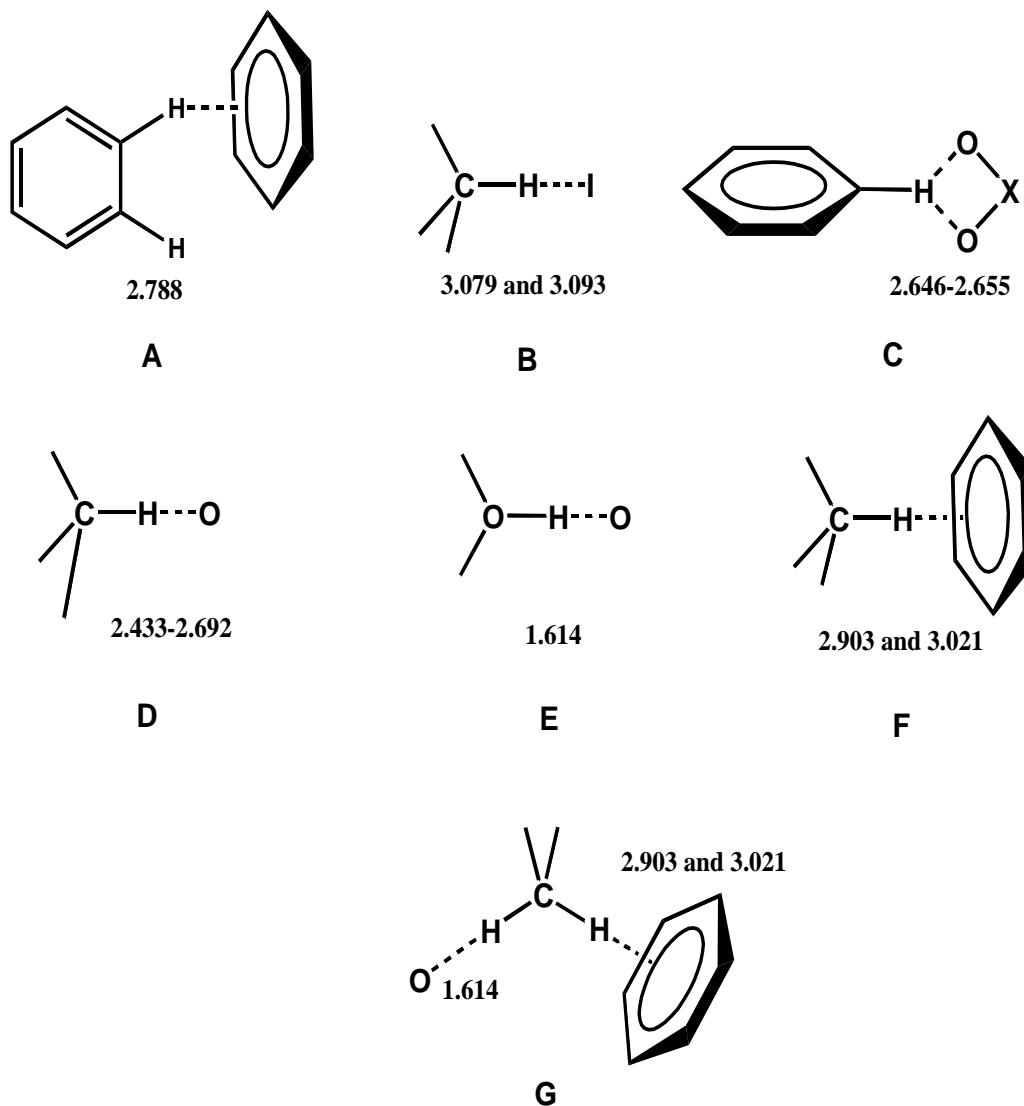
Compound 1			
Bond distances (Å)		Bond angles (°)	
S1—O3	1.440 (3)	O3—S1—O2	112.2 (2)
S1—O4	1.443 (3)	O4—S1—O2	113.8 (2)
S1—O2	1.460 (2)	O3—S1—O1	107.89 (18)
S1—O1	1.569 (2)	O2—S1—O1	101.83 (12)
N11—C111	1.486 (6)	C111—N11—C121	109.4 (4)
N11—C121	1.501 (4)	C111—N11—C131	107.9 (4)
N11—C11	1.507 (3)	C111—N11—C11	111.2 (4)
C11—C16	1.371 (6)	C16—C11—C12	120.7 (3)
C12—C13	1.409 (7)	C16—C11—N11	119.8 (4)
C13—C14	1.345 (8)	C11—C12—C13	116.9 (5)
C14—C15	1.385 (7)	C14—C13—C12	122.3 (5)
Compound 2			
Bond distances (Å)		Bond angles (°)	
N11—C1	1.499 (3)	C11—N11—C12	108.3 (2)
N11—C11	1.510 (3)	C1—N11—C13	110.87 (19)
N11—C12	1.511 (3)	C1—N11—C11	111.9 (2)
C1—C2	1.383 (4)	C6—C1—N11	118.4 (2)
C2—C3	1.390 (4)	C2—C1—N11	121.4 (2)
C3—C4	1.384 (4)	C1—C2—C3	119.7 (3)

Table 3 : Hydrogen bond parameters (Å, °) for **1** and **2**.

D—H...A	D—H	H...A	D...A	D-H...A
Compound 1				
C11—H11A...I1	0.96	3.079	4.010	164
C6—H6...I1#1	0.93	3.093	3.972	158
C5—H5#2...C _g	0.93	2.788	3.619	149
Compound 2				
S1—O1—H1#1...O2	0.99	1.614	2.603	176
S1—O1...H14	0.967	2.646	3.474	144
S1—O2...H14	0.967	2.655	3.532	151
S1—O3...H13B#2	0.951	2.433	3.345	161
S1—O4...H11A#3	1.01	2.516	3.400	146
S1—O2...H16#4	0.989	2.607	3.366	134
S1—O3...H12A#4	1.05	2.509	3.526	163
S1—O3...H16#4	0.989	2.612	3.403	137
S1—O4...H12B#5	0.907	2.692	3.436	140
S1—O4...H13A#5	0.94	2.554	3.446	159
C12-H12B...C _{g1}	0.91	2.903	3.453	121
C11-H11B...C _{g1}	0.97	3.021	3.954	162

Symmetry codes: #1 $x-1/2, 3/2-y, z$; #2 $x, 1+y, z$; #3 $x, 1+y, z$; #4 $-x, 1-y, -1/2+z$; #5 $-x, 1-y, 1/2+z$. C_g: ring C1/C2/C3/C4/C5/C6
 C_{g1}: rings C11-C16

The hydrogen atoms of the methyl groups form simultaneously two types of interactions, $\text{H}_2\text{C}-\text{H}\dots\text{O}$ contacts (2.433-2.692 Å), Synthons **D**, and $\text{H}_2\text{C}-\text{H}\dots\pi$ contacts, Synthons **F**, with $\text{H}_2\text{C}-\text{H}\dots\text{C}_g$ distances of 2.903 and 3.021 Å to support the $\text{O}-\text{H}\dots\text{O}$ (1.614 Å) hydrogen-bonds between bisulfate anions (Scheme 2; Synthons **E**). Therefore, the methyl group involved in these two contacts shows a distinct supramolecular Synthons **G**, Scheme 2.



Scheme 2: Classical and non-classical hydrogen-bonding synthons found in (1) and (2). Distances (in Å) are shown within each motif. References for the different supramolecular motifs are as follows: A,^[8] B, C, D and E,^[3-5] F.^[10]

The extended structure of 1 and 2: Crystal packing and supramolecular structures

The crystallographic independent TMPA^+ cations occur in layers of embraced phenyl rings, with I^- anions arranged in between the cation layers. The cations layers are embraced through aryl...aryl edge-to-face motifs of the contacts $\text{C}-\text{H}\dots\text{C}_g$ (2.788 Å), (scheme 2, synthon **A**), Figure 2. The anion chains connect the cation layers through $\text{H}_2\text{C}-\text{H}\dots\text{I}$ interactions in the c-direction leading to 3D network, Figure 3.

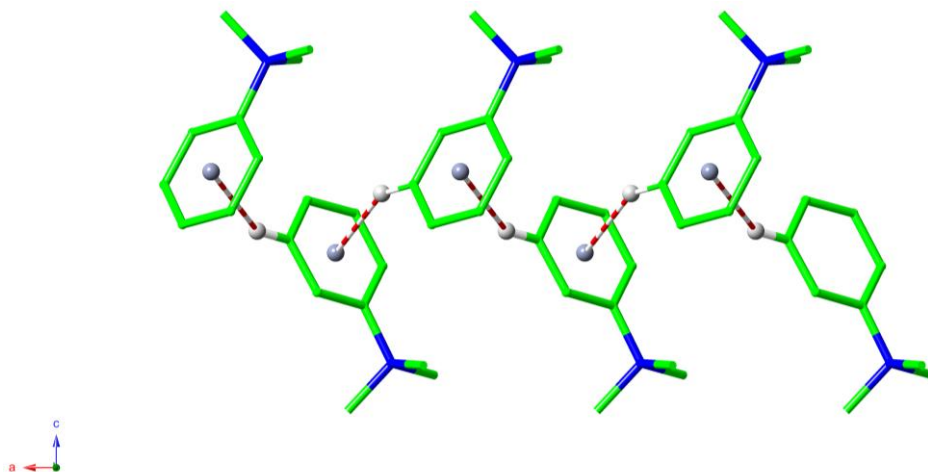


Fig. 2: The diagram showing one layer of aryl...aryl embraced TMPA cations to emphasize the orientation of the supramolecular synthon that results from the edge-to-face supramolecular motif of C—H... π interactions. The C—H... π interactions are shown as rendered multi-band cylinders, hydrogen atoms and ring centroids are represented as spheres (other C-H atoms were omitted for clarity).

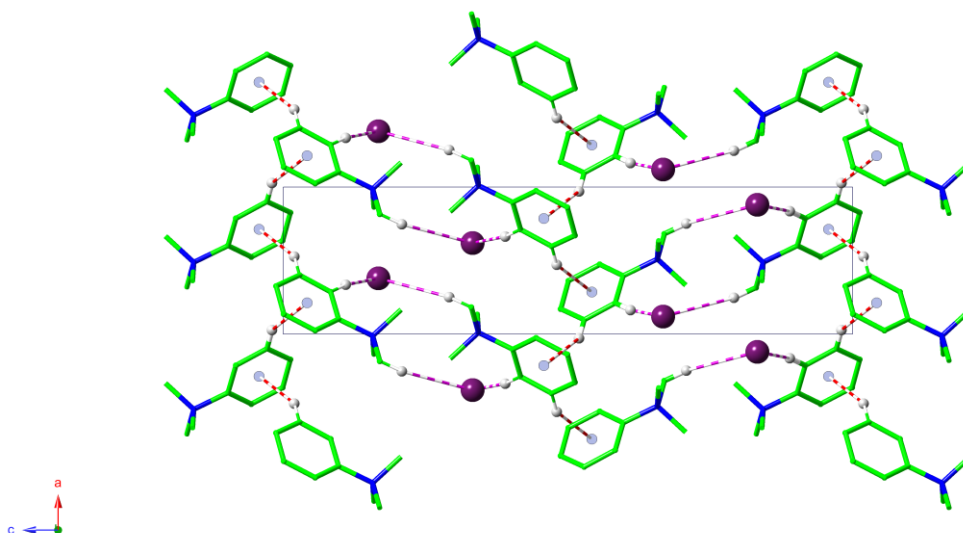


Fig. 3: Overall packing diagram of **1**; iodide ions, ring centroids and hydrogen atoms involved in interactions appear as spheres and H₂C—H...I and C—H... π interactions are shown as rendered multi-band cylinders (other C-H atoms were omitted for clarity).

The crystal structure of **2** is dominated by C—H...O interactions. The HSO₃[−] anions interact via O—H...O intermolecular interactions (1.614 Å) leading to zig-zag chains parallel to the *a* crystallographic axis, Figure 4. Parallel to these chains the TMPA cations on the other hand are assembled in organic chains through C—H... π interaction represented by the H₂C—H...C_g interactions which are evident by the short distances of 2.903 and 3.021 Å, Table 3. The anion chains and the cation chains are further connected to each other by extensive hydrogen bond interactions into sheets in the *ab* plane, Figure 5. These interactions and the symmetry related ones in **2**, and the H₂C—H...O interactions in the *c* direction result in the three-dimensional overall packing diagram, Figure 6. The overall packing diagram therefore shows the chains

arranged where each chain is surrounded by four other chains of the counter ion. The geometrical parameters of these interactions are listed in Table 3.

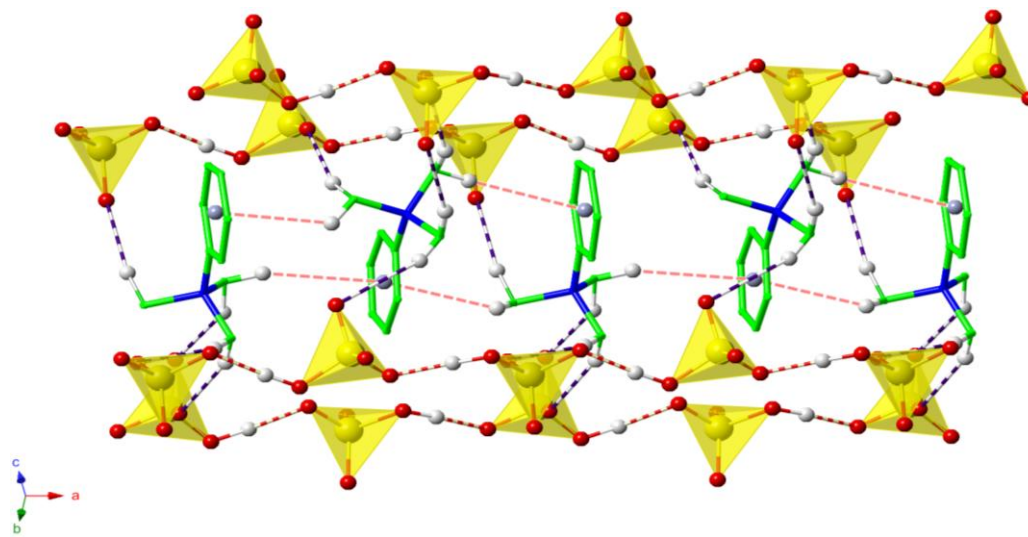


Fig. 4: Cations chains formed via $\text{H}_2\text{C}-\text{H}\dots\pi$ and anion chains assembled via $\text{O}-\text{H}\dots\text{O}$ interactions of **2**; contact atoms and ring centroids involved in interactions appear as spheres and $\text{H}_2\text{C}-\text{H}\dots\pi$ and $\text{O}-\text{H}\dots\text{O}$ interactions are shown as rendered multi-band cylinders (other C-H atoms were omitted for clarity).

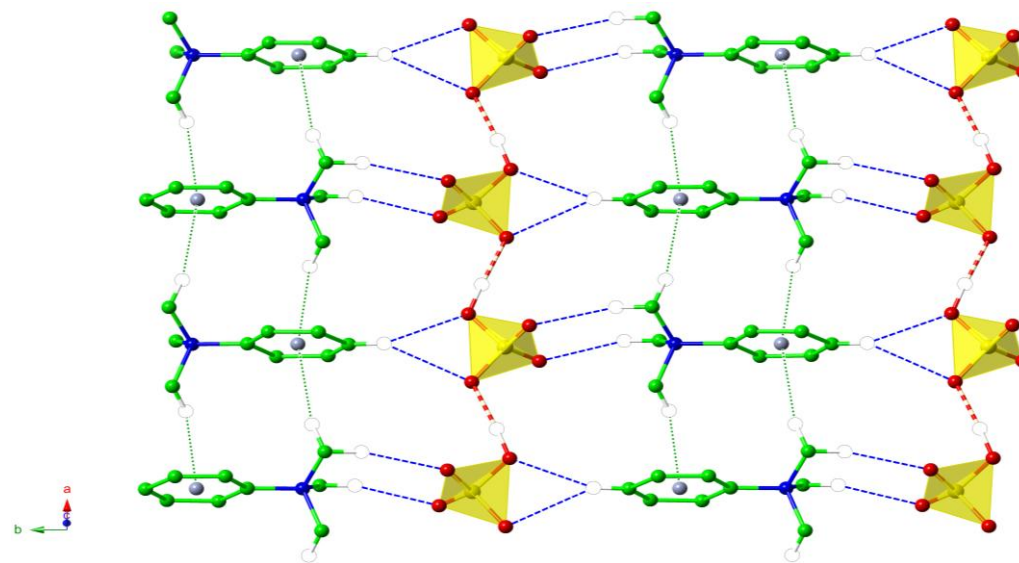


Fig. 5: One sheet of interacting cations and anions chains of **2**. Extensive $\text{H}_2\text{C}-\text{H}\dots\pi$, $\text{C}-\text{H}\dots\text{O}$ and $\text{O}-\text{H}\dots\text{O}$ interactions are shown as rendered multi-band cylinders (other C-H atoms were omitted for clarity).

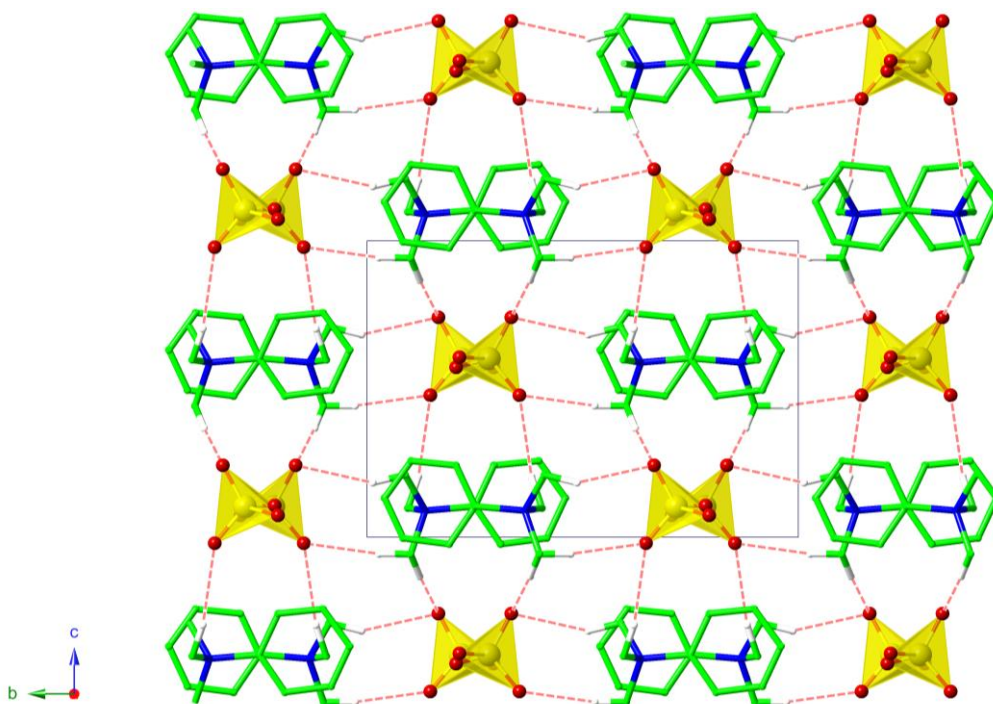


Fig. 6: Overall packing diagram of **2**. Bisulfate anions appear as polyhedral while cations are in stick presentation. The diagram shows the arrangement of cations layers and anions chains that are connected through extensive hydrogen bonding. Each cation layer is surrounded by four anion chains and vice versa (other C-H atoms were omitted for clarity).

Concluding remarks

The crystal and molecular structures of the trimethylphenyammonium salts, [TMPA]⁺Γ⁻ (**1**) and [TMPA]⁺(HSO₄⁻) (**2**) have been determined and compared. Some features are:

1. The compounds crystallize in orthorhombic crystal structures.
2. Compound **1** shows both H₂C—H...I and C—H...π hydrogen bonding interactions. Introducing the hydrogen sulfate anion in **2** allows more predominant O—H...O hydrogen bonding along with non-classical C—H... π hydrogen bonding.
3. The C—H...π interactions appear in different motifs. In **1**, it is in edge-to-face phenyl...phenyl interactions, while, it is H₂C—H...phenyl interactions in **2**.
4. Lattices of both **1** and **2** consolidate supramolecular structures.

Acknowledgement

The authors thank Al al-Bayt University for financial support.

Supplementary material

CCDC 1415201 and 1415202 contain the supplementary crystallographic data for salts **1** and **2**. These data can be obtained free of charge via <http://www.ccdc.cam.ac.uk/conts/retrieving.html>, or from the Cambridge Crystallographic Data Centre, 12 Union Road, Cambridge CB2 1EZ, UK; fax: (+44) 1223-336-033; or e-mail: deposit@ccdc.cam.ac.uk.

References

- [1] Müller-Dethlefs, K.; Hobza, P., *Chem. Rev.*, 1999, 100, 143.
- [2] Johnson, E. R.; Keinan, S.; Mori-Sánchez, P.; Contreras-García, J.; Cohen, A. J.; Yang, W., *J. Am. Chem. Soc.*, 2010, 132, 6498.
- [3] Scheiner, S., *Hydrogen bonding, A theoretical perspective*. Oxford University Press, New York, 1997.
- [4] Desiraju, G. R., *Acc. Chem. Res.*, 2002, 35, 565.
- [5] Steiner, T., *Angew. Chem. Int. Ed.* 2002, 41, 48.
- [6] Lieberman, H. F.; Davey, R. J.; Newsham, D. M. T., *Chem. Mater.*, 2000, 12, 490.
- [7] Dance, I., *New J. Chem.*, 2002, 27, 22.
- [8] Dance, I., *Supramolecular Inorganic Chemistry, in The Crystal as a Supramolecular Entity*, John Wiley & Sons, Ltd, New York, 1996; p 137.
- [9] Nangia, A.; Desiraju, G. R., *Topics in Current Chemistry*, Vol. 198, edited by E. Weber, Berlin Heidelberg, Springer Verlag, 1998.
- [10] Nishio, M.; Hirota, M.; Umezawa, Y., *The CH-[pi] interaction: Evidence, Nature, and Consequences*. Wiley-VCH, New York, 1998, Vol. 21.
- [11] Nepal, B.; Scheiner, S., *J. Phys. Chem. A*, 2014, 118, 9575.
- [12] Torrice, M. M.; Bower, K. S.; Lester, H. A.; Dougherty, D. A., *Proc. Natl. Acad. Sci.*, 2009, 106, 11919.
- [13] Gromiha, M. M., *Biophys. Chem.*, 2003, 103, 251.
- [14] Dupont, J.; Suarez, P. A.; De Souza, R. F.; Burrow, R. A.; Kintzinger, J. P., *Chem. Eur. J.*, 2000, 6, 2377.
- [15] Yamada, S.; Iwaoka, A.; Fujita, Y.; Tsuzuki, S., *Org. Lett.*, 2013, 15, 5994.
- [16] Abu-Salem, Q. *J. Chem. Crystallogr.*, *In press*.
- [17] Kuhn, N.; Abu-Salem, Q.; Gädt, T.; Reit, R.; Steimann, M., *Z. Naturforsch.*, 2007, 62b, 871.
- [18] Kuhn, N.; Abu-Salem, Q.; Maichle-Mößmer, C.; Steimann, M., *Z. Anorg. Allg. Chem.* 2007, 633, 683.
- [19] Abu-Salem, Q., *Synth. React. Inorg. Met.-Org. Chem.*, 2016, 46, 821.
- [20] Sheldrick, G. M., *SHELXL-97 Programs for Crystal Structure Refinement*, University of Göttingen, Germany, 1997.
- [21] Sommer, H. Z.; Jackson, L. L., *J. Org. Chem.*, 1970, 35 (5), 1558.
- [22] Oba, A.; Hashimoto, M., *Acta Cryst. E*, 2012, 68, m1467.
- [23] Keng, T. C.; Lo, K. M.; Ng, S. W., *Acta Cryst. E*, 2011, 67, m872.
- [24] Lo, K. M.; Ng, S. W., *Acta Cryst. E*, 2010, 66, m166.
- [25] Lo, K. M.; Ng, S. W., *Acta Cryst. E*, 2010, 66, m353.
- [26] Bond, M., *Acta Cryst. C*, 2010, 66, m17.
- [27] Yap, Q. L.; Lo, K. M.; Ng, S. W., *Acta Cryst. E*, 2009, 65, m714.
- [28] deGeorge, J.; Landee, C. P.; Turnbull, M. M., *Acta Cryst. E*, 2013, 69, o471.
- [29] Damous, M.; Denes, G.; Bouacida, S.; Hamlaoui, M.; Merazig, H.; Daran, J.-C., *Acta Cryst. E*, 2013, 69, o1458.
- [30] Thanigaimani, K.; Khalib, N. C.; Arshad, S.; Razak, I. A., *Acta Cryst. E*, 2013, 69, o42.
- [31] Mammadova, G. Z.; Matsulevich, Z. V.; Borisova, G. N.; Borisov, A. V.; Khrustalev, V. N., *Acta Cryst. E*, 2013, 69, o703.